Trivalent Actinide and Lanthanide Complexation of 5,6-Dialkyl-2,6-bis(1,2,4-triazin-3-yl)pyridine (RBTP; R = H, Me, Et) Derivatives: A Combined Experimental and First-Principles Study

Arunasis Bhattacharyya,*[,†,‡] Eunja Kim,[§] Philippe F. Weck,[⊥] Paul M. Forster,[†] and Kenneth R. Czerwinski[†]

[†]Department of Chemistry, University of Nevada—Las Vegas, Las Vegas, Nevada 89154, United States
[‡]Radiochemistry Division, Bhabha Atomic Research Centre, Trombay, Mumbai 400-085, India
[§]Department of Physics and Astronomy, University of Nevada—Las Vegas, Las Vegas, Nevada 89154, United States
[⊥]Sandia National Laboratories, Albuquerque, New Mexico 87185-0747, United States

S *Supporting Information*
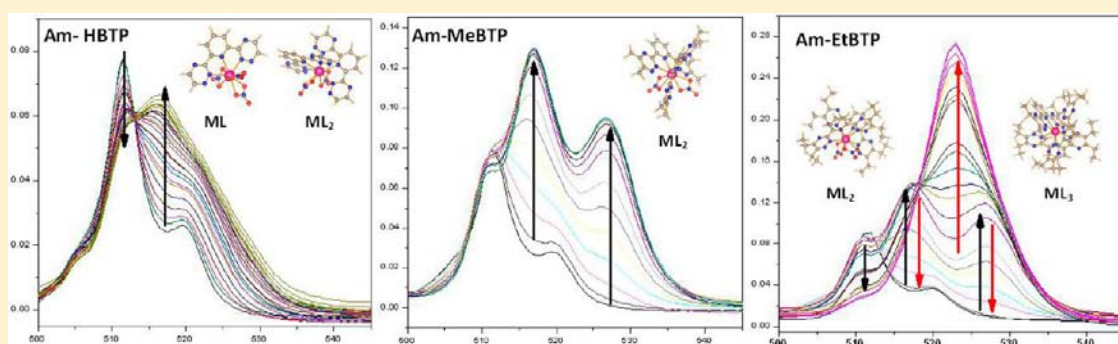
ABSTRACT: Complexations of lanthanide ions with 5,6-dialkyl-2,6-bis(1,2,4-triazin-3-yl)pyridine [RBTP; R = H (HBTP), methyl (MeBTP), ethyl (EtBTP)] derivatives have been studied in the acetonitrile medium by electrospray ionization mass spectrometry, time-resolved laser-induced fluorescence spectroscopy, and UV—vis spectrophotometric titration. These studies were carried out in the absence and presence of a nitrate ion in order to understand the effect of the nitrate ion on their complexation behavior, particularly in the poor solvating acetonitrile medium where strong nitrate complexation of hard lanthanide ions is expected. Consistent results from all three techniques undoubtedly show the formation of lower stoichiometric complexes in the presence of excess nitrate ion. This kind of nitrate ion effect on the speciation of Ln^{3+} complexes of RBTP ligands has not so far been reported in the literature. Different Am^{3+} and Ln^{3+} complexes were observed with RBTP ligands in the presence of 0.01 M tetramethylammonium nitrate, and their stability constant values are determined using UV—vis spectrophotometric titrations. The formation of higher stoichiometric complexes and higher stability constants for Am^{3+} compared to Ln^{3+} ions indicates the selectivity of these classes of ligands. A single-crystal X-ray diffraction (XRD) study of europium(III) complexes shows the formation of a dimeric complex with HBTP and a monomeric complex with EtBTP, whereas MeBTP forms both the dimeric and monomeric complexes. Density functional theory calculations confirm the findings from single-crystal XRD and also predict the structures of Eu^{3+} and Am^{3+} complexes observed experimentally.

1. INTRODUCTION

There is significant covalent contribution in the d-block transition-metal complexes, whereas the bonding in the f-element complexes is mainly governed by the ionic interaction. The complexing ability of the f elements is, therefore, dictated by their ionic potential.[1,2] Lighter actinides (up to plutonium) show multiple oxidation states, and separation methods can be designed by tuning their oxidation states, as implemented in the well-known PUREX process. The transplutonides, however, are trivalent, and their complexation behavior is very similar to the trivalent lanthanides because of their similar ionic potential.[3] Trivalent minor actinides are produced in a nuclear reactor as the activation products of uranium and plutonium, whereas the

lanthanides are their fission products. The separation of trivalent actinides (An^{3+}) and lanthanides (Ln^{3+}) is, therefore, a challenging task in the nuclear fuel cycle. Ln^{3+}/An^{3+} separation is, however, essential prior to the transmutation of the long-lived, highly radiotoxic minor actinides because of the very large neutron absorption cross section of some of the lanthanide isotopes.[4] The actinides possess 5f valence orbitals with higher spatial distribution compared to the 4f orbitals of the lanthanides. This leads to the formation of stronger covalent bonds of the actinides with the soft donor ligands

compared to that of the lanthanides.[5] This property of the f-block elements is being exploited for intergroup separation of trivalent actinides and lanthanides. A number of S- and N-donor ligands have been investigated for Ln^{3+}/An^{3+} separation.[6] Among various N-donor ligands studied in the literature, 2,6-bis(1,2,4-triazinyl)pyridine (BTP) derivatives show quite promising results.[7,8] The complexation behavior of the BTP derivatives is affected significantly with changes in the alkyl substituents because different stoichiometric complexes have been isolated by varying the alkyl substituents.[9,10] A single-crystal X-ray diffraction (XRD) study showed the formation of an unusual 12-coordinated lanthanide (Ln^{3+}) complex of unsubstituted BTP (HBTP; Figure 1a) from the acetonitrile
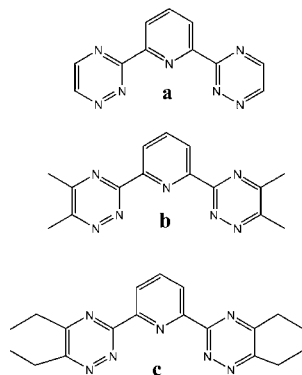
Figure 1. RBTP ligands studied in the present work: (a) HBTP; (b) MeBTP; (c) EtBTP.

medium.[9] Only one report on the solution-phase Ln^{3+} complexation of HBTP, however, shows the formation of a 1:1 complex in a methanol/water mixture,[11] which cannot explain the formation of the 12-coordinated solid complex $Ln(HBTP)_2(NO_3)_3$.[9] No literature is available on the solution-phase complexation study of lanthanides with this simplest BTP molecule in acetonitrile, which will be interesting to study in view of the formation of an unusal solid complex in this medium. The presence of a nitrate ion is expected in the solution to be treated for the separation of trivalent actinides and lanthanides in the nuclear fuel cycle.[6] The nitrate ion can strongly affect the complexation behavior of the 5,6-dialkyl-2,6-bis(1,2,4-triazin-3-yl)pyridine [RBTP; R = H (HBTP), methyl (MeBTP), ethyl (EtBTP)] ligands because of the strong complexing nature of the nitrate ions toward the lanthanides and actinides.[12] Literature studies on RBTP complexation with Ln^{3+} and An^{3+} were carried out at a fixed ionic strength.[13−15] There is, however, no clear picture on how the presence of nitrate ion can alter the complexation behavior of this class of ligands. It will, therefore, be of interest to study the complexation of these "f"-block elements with RBTP derivatives in the absence and presence of excess nitrate ion particularly in a weakly solvating acetonitrile medium, where higher nitrate complexation is expected. A systematic study is, therefore, performed on the complexation of Ln^{3+} ions with RBTP in the acetonitrile medium in the absence and presence of 0.01 M tetramethylammonium nitrate (TMAN) using electrospray ionization mass spectrometry (ESI-MS), time-resolved laser-induced fluorescence spectroscopy (TRLFS), and UV−vis spectrophotometric titration. Stronger Am^{3+} complexation with a similar tridentate N-donor ligand, 2-amino-4,6-di(pyridine-2-yl)-1,3,5-triazine, compared to the

Ln^{3+} ions is reported in the literature.[16] Stronger Cm^{3+} complexation with RBTP compared to Ln^{3+} with this class of ligands has been reported by determining the stability constants of their complexes using the TRLFS technique.[15] Denecke et al. did not observe any significant structural difference in the 1:3 RBTP complexes of Am^{3+}, Cm^{3+}, and Ln^{3+} ions from an extended X-ray absorption fine structure study.[17,18] To the best of our knowledge, only one literature is available on the complexation study of Am^{3+} with MeBTP in a methanol/water mixture.[19] No literature is available on the systematic study on Am^{3+} complexation with RBTP ligands with various R groups. Am^{3+} complexation is, therefore, studied with HBTP, MeBTP, and EtBTP derivatives using UV−vis spectrophotometric titration in the acetonitrile medium at 0.01 M fixed ionic strength in order to understand the role of alkyl substituents on the complexation behavior. The stability constants of various lanthanide ions and Am^{3+} with all three ligands in the acetonitrile medium in the presence of 0.01 M TMAN have been determined from the UV−vis spectrophotometric titrations in order to have the quantitative idea about the distribution of the species and to understand the reason for the selectivity of this class of ligands toward the trivalent actinide ions. A single-crystal XRD study was carried out on the europium(3+) complexes of all three RBTP ligands in the solid phase to understand the role of the alkyl substituent on the structure of the complexes.

2. EXPERIMENTAL SECTION

2.1. Reagents and Chemicals. All three N-donor ligands RBTP (HBTP, MeBTP, and EtBTP) were synthesized according to the literature-reported method. HBTP was synthesized in high yield by stirring the trimeric glyoxal with 2,6-pyridinecarboxamide hydrazone in dry methanol at room temperature for 3 h under nitrogen followed by overnight refluxation. The desired compound was obtained by filtering the yellow solid precipitate.[9] MeBTP and EtBTP were, however, synthesized by refluxing 1.0 equiv of 2,6-pyridinecarboxamide hydrazone with 2.1 equiv of 2,3-butandione and 3,4-hexanedione, respectively, in an ethanol medium. Pure product was obtained by recrystallizing the yellowish solid from an ethanol medium.[20] All three ligands were characterized by ^{1}H NMR, ESI-MS, and melting point measurements, which corroborates nicely with the literature reports. High-purity crystals of $Ln(NO_3)_3 \cdot nH_2O$ (n = 5 or 6) from Sigma-Aldrich were used to prepare appropriate solutions in high-performance liquid chromatography grade acetonitrile (100%) or methanol in the absence and presence of TMAN (Sigma-Aldrich).

2.2. ESI-MS. ESI-MS measurements were performed on a Dionex MSQ plus ESI with a quadrupole mass filter detector. The solution samples were introduced in a capillary (10 μL) and then were diluted in a carrier solvent (100% acetonitrile HPLC grade), which ends in a very fine tip where a high voltage was applied (30 kV) with a temperature of 350 °C and the sample cone voltage was set at 30 V. The solvent was completely evaporated into the evaporation chamber, and the droplets split up to the point that each droplet was a single charged molecule. According to the polarity chosen (negative or positive), the mass filter detector was able to detect respectively negative, positive, or neutral compounds.

2.3. Steady-State Fluorescence Study. A steady-state fluorescence study was carried out using a Horiba-Jobin Yvon Fluorolog 3 spectrofluorimeter where a xenon lamp was the excitation source. The excitation wavelength (λ_{ex}) of 394 nm was chosen to excite the europium(3+) complexes, and the emission window selected was 500−750 nm with excitation and emission slit widths of 5 and 1 nm, respectively.

2.4. TRLFS Study. The TRLFS system was used to determine the fluorescence lifetime. The VIBRANT laser system (OPOteck, Inc., Carlsbad, CA) uses the third harmonic of a Nd:YAG laser to pump an optical parametric oscillator (OPO). The OPO then produces an
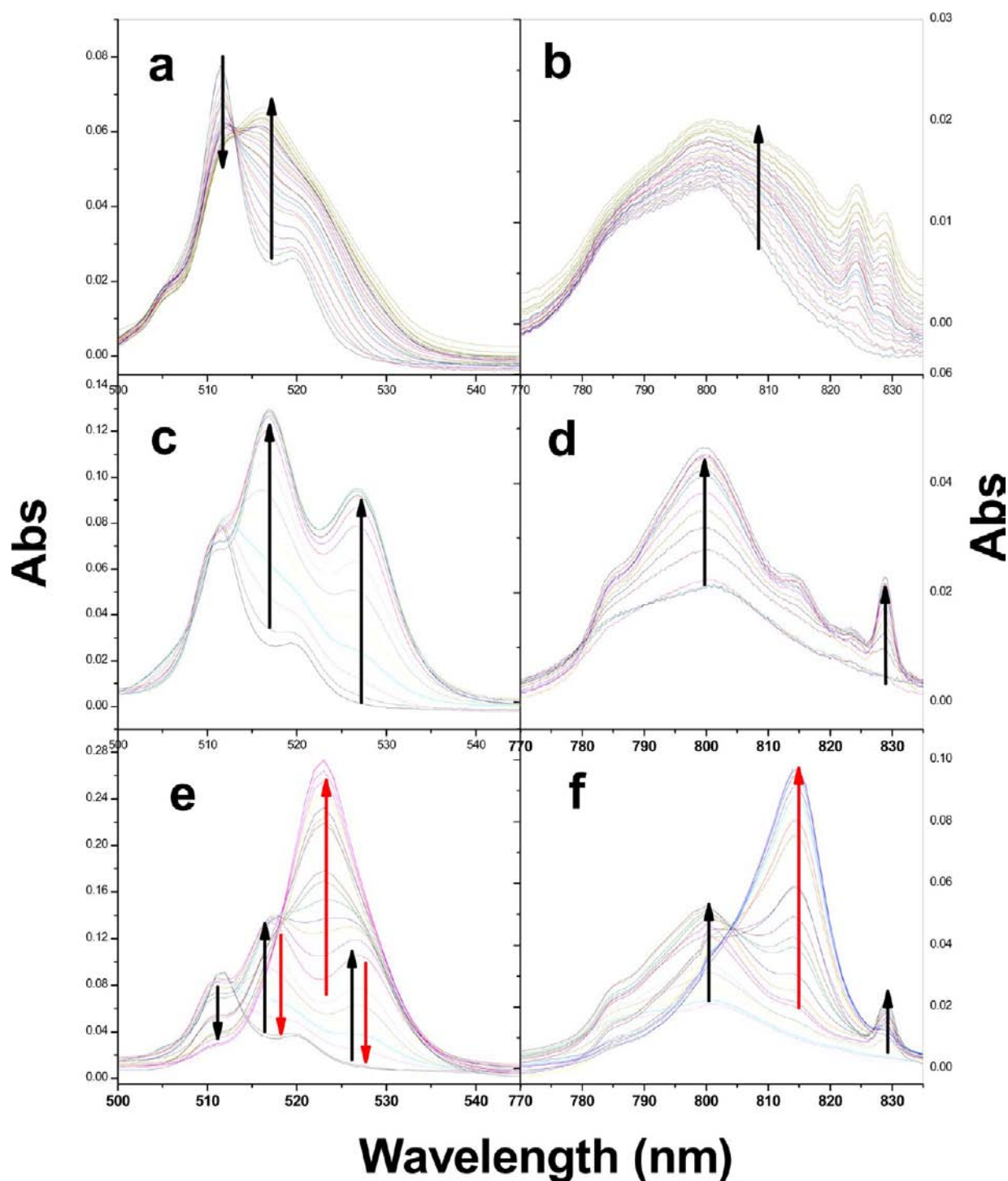
Figure 2. Titration profile of 0.6 mM Am(NO$_3$)$_3$ with a 10 mM solution of HBTP (a and b), MeBTP (c and d), and EtBTP (e and f) in the acetonitrile medium in the presence of 0.01 M TMAN.

excitation beam with wavelengths between 300 and 2400 nm. The excitation beam is then focused through a periscope assembly from Thor Laboratories to adjust the beam height. The beam passes through a 92/8 pellicle beam splitter. The lesser split is collected on a PE25 pyroelectric power meter (Ophir Inc.). Sample fluorescence is focused onto a PI-MAX II CCD detector (Roper Scientific/Princeton Instruments, Trenton, NJ) by means of a SP500 spectrograph (Roper Scientific) with an entrance slit width of 250 μm. The laser system outputs ~25 mJ/pulse at 410 nm and ranges down to less than 1 mJ/pulse in the near-IR (NIR). A frequency-doubling UV module was inserted in order to excite the solution containing europium(3+)

complexes at 394 nm. Measurement of the fluorescent signals after the excitation pulse as well as measurement of the species lifetimes was controlled by the PI-MAX timing generator. The fluorescence spectra were recorded from 560 to 640 nm with a 600 g/mm, 500 nm BLZ grating after a delay time of 1.2 μs to discriminate the short-lived fluorescence of the organic ligands. Every measurement is triggered by a signal sent from the laser control hardware (Q-Switch Synchro) to the timing generator, indicating that the laser has fired.

2.5. UV−Vis Spectrophotometric Titration. Spectrophotometric titrations for the Ln^{3+} ions were carried out with a Cary 6000i UV−vis−NIR spectrophotometer by following the π−π* absorption bands

of RBTP in the wavelength range 250−450 nm. The solution of different RBTP ligands (1.0×10^{-4} M) in the acetonitrile medium was titrated with a lanthanide(III) solution (4.0×10^{-4}−2.0×10^{-3} M) until variation in the absorption spectra became negligible, whereas in the case of Am^{3+} complexation studies, an $Am(NO_3)_3$ (6.0×10^{-4} M) solution was titrated with RBTP (1.0×10^{-2} M) in the acetonitrile medium. In all of the UV−vis spectrophotometric titrations, a fixed ionic strength of 0.01 M was maintained using TMAN. The stability constant values for Ln^{III}-RBTP (log β_{xy}) were calculated from the change in the UV−vis absorption spectra of the ligand over the wavelength range of 250−450 nm, and those for Am^{III}-RBTP were calculated from the change in americium(III) spectra on complexation in the wavelength ranges 500−540 nm (Figure 2a,c,e) and 775−835 nm (Figure 2b,d,f) using Hypspec.[21,22] The absorption spectra recorded during titration of MeBTP with europium(III) are shown
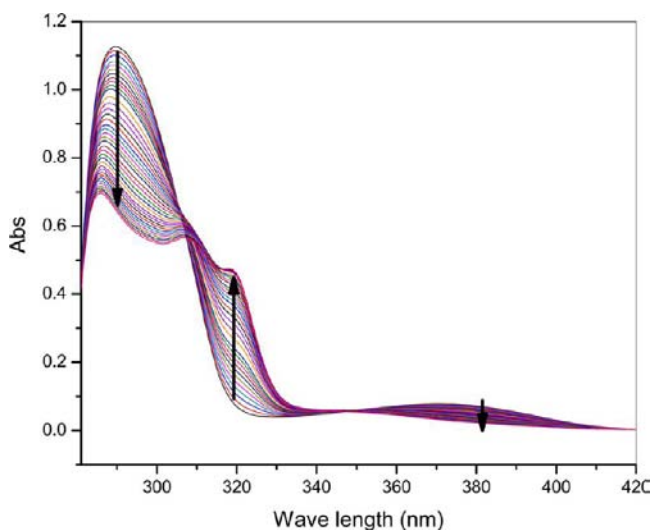
Figure 3. UV−vis spectrophotometric titration of MeBTP (1.0×10^{-4} M) by $EuNO_3$ (4×10^{-4} M) in the acetonitrile medium in the presence of 0.01 M TMAN.

in Figure 3. The absorbance $[A^i(\lambda)]$ at a particular wavelength (λ) for the ith injection can be expressed as (Lambert−Beer's law)

$$A^i(\lambda) = l \sum \varepsilon_j(\lambda) \, C_j^i \tag{1}$$

where $\varepsilon_j(\lambda)$ is the molar absorbance of the jth species and C_j^i is the concentration of the jth species at the ith injection. These equations in combination with mass balance equations (3) and (4) were solved using Hypspec to obtain the log β_{xy} as well as free equilibrium concentrations of different species.

$$x\text{M} + y\text{L} = \text{M}_x\text{L}_y \qquad \log \beta_{xy} \tag{2}$$

$$C_M^T = [\text{M}] + \sum x\beta_{xy}[\text{M}]^x[\text{L}]^y \tag{3}$$

$$C_L^T = [\text{L}] + \sum y\beta_{xy}[\text{M}]^x[\text{L}]^y \tag{4}$$

where C_L^T and C_M^T are the total concentrations of ligand and metal ions, respectively, and $[\text{L}]$ and $[\text{M}]$ are the respective equilibrium concentrations. Several chemically possible species (M_xL_y, where $x = 1$−2 and $y = 1$−3) were submitted as input to Hypspec. However, the software program consistently converged (lowest χ^2) with the specific set of metal complex species only. The molar absorbances of free MeBTP and its different europium(3+) complexes, obtained from Hypspec, are plotted in Figure 4, and those of free americium(III) and its complexes of HBTP, MeBTP, and EtBTP are plotted in Figure 5.

2.6. Single-Crystal XRD Studies. *Preparation of Europium(3+) Complexes.* $[Eu_2(HBTP)_2(NO_3)_6]\cdot2CH_3CN$ (*1*). To a stirred solution of
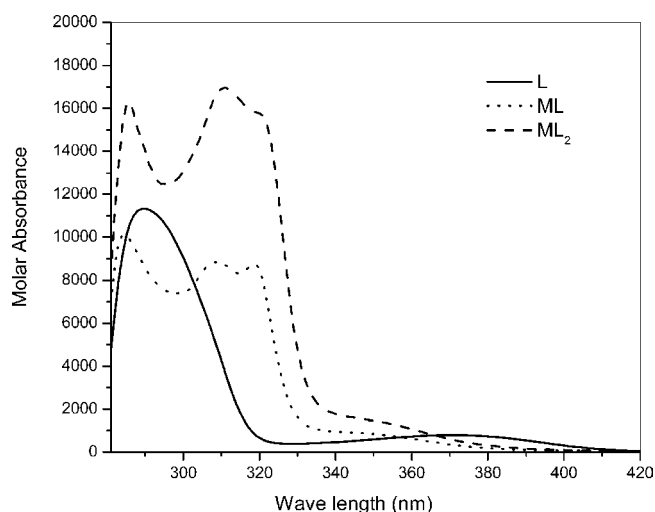
Figure 4. Molar absorbance of MeBTP and its 1:1 and 1:2 complexes of europium(III) in acetonitrile with 0.01 M TMAN obtained by fitting the UV−vis spectrophotometric titration data using Hypspec.
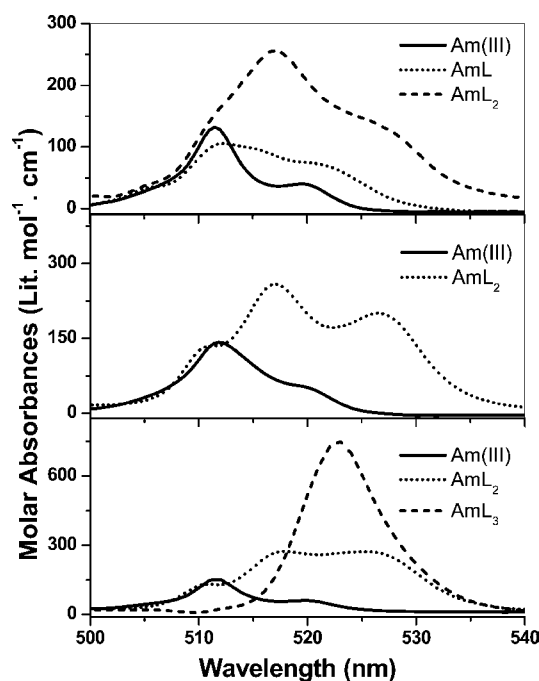
Figure 5. Molar absorbance of americium(III) and its complexes with HBTP, MeBTP, and EtBTP in am acetonitrile medium in the presence of 0.01 M TMAN.

$Eu(NO_3)_3\cdot5H_2O$ (0.05 mmol) in acetonitrile (3 mL) was added dropwise a solution of HBTP (0.05 mmol) in acetonitrile (3 mL). The solution was stirred for 30 min and filtered. Crystals suitable for X-ray crystallography were obtained after slow evaporation of the solvent for several days. Calc for $Eu_2C_{26}H_{20}N_{22}O_{18}$: C, 25.34; H, 1.64; N, 25.00. Found: C, 25.23; H, 1.69; N, 25.21.

[Eu(MeBTP)(NO₃)₃(H₂O)]·CH₃CN (2a) and [Eu₂(MeBTP)₂(NO₃)₆] (2b). To a stirred solution of $Eu(NO_3)_3\cdot5H_2O$ (0.05 mmol) in acetonitrile (3 mL) was added dropwise a solution of MeBTP (0.05 mmol) in acetonitrile (3 mL). The solution was stirred for 30 min and filtered. Two different types of crystals of **2a** and **2b** could be isolated after slow evaporation of the solvent for several days. Calcd for $EuC_{17}H_{20}N_{11}O_{10}$: C, 29.58; H, 2.92; N, 22.32. Calcs for $Eu_2C_{26}H_{20}N_{22}O_{18}$: C, 28.54; H, 2.39; N, 22.19. Found: C, 28.79; H, 2.55; N, 22.25.

Table 1. Summary of Crystallographic Data Collection and Refinement for the Europium(III) Complexes of RBTP

	europium(III) complex			
	1	**2a**	**2b**	**3**
formula	$[Eu_2(HBTP)_2(NO_3)_6]\cdot2CH_3CN$	$[Eu(MeBTP)(NO_3)_3,H_2O]\cdot CH_3CN$	$[Eu_2(MeBTP)_2(NO_3)_6]$	$[Eu(EtBTP)(NO_3)_3,H_2O]\cdot CH_3CN$
empirical formula	$Eu_2C_{26}\ H_{20}\ N_{22}\ O_{18}$	$Eu\ C_{17}\ H_{20}\ N_{11}\ O_{10}$	$Eu_2C_{30}\ H_{30}\ N_{20}\ O_{18}$	$EuC_{21}\ H_{28}\ N_{11}\ O_{10}$
fw	1232.56	690.40	1262.66	746.50
T (K)	100(2)	100(2)	100(2)	100(2)
cryst syst	triclinic	triclinic	monoclinic	triclinic
space group	$P\bar{1}$	$P\bar{1}$	$P2(1)/n$	$P\bar{1}$
unit cell dimens				
a (Å)	9.5679(5)	8.4739(4)	13.1674(8)	7.8334(14)
b (Å)	11.3093(6)	12.6134(7)	10.8952(6)	9.8055(18)
c (Å)	11.4263(6)	12.7731(7)	15.3985(9)	18.715(3)
α (deg)	61.3650(10)	92.7810(10)	90	85.963(3)
β (deg)	73.8480(10)	102.8820(10)	106.6330(10)	87.125(3)
γ (deg)	73.1370(10)	106.5610(10)	90	84.520(3)
V (Å^3)	1024.16(9)	1266.47(12)	2116.7(2)	1426.1(4)
Z	1	2	2	2
density (calcd) (Mg/m^3)	1.998	1.810	1.981	1.739
abs coeff (mm^{-1})	3.137	2.550	3.037	2.272
$F(000)$	600	684	1240	748
cryst size (mm^3)	$0.2 \times 0.04 \times 0.04$	$1 \times 0.08 \times 0.08$	$0.1 \times 0.02 \times 0.02$	$0.12 \times 0.06 \times 0.06$
θ range for data collection (deg)	2.06−30.51	2.22−30.51	2.32−26.37	2.09−30.51
reflns collected	16735	20684	24926	8615
indep reflns	6222 [R(int) = 0.0194]	7694 [R(int) = 0.0188]	4333 [R(int) = 0.0352]	8615 [R(int) = 0.0000]
data/restraints/param	6222/0/308	7694/0/358	4333/0/320	8615/0/394
GOF on F^2	1.042	1.069	1.072	1.111
final R indices [$I > 2\sigma(I)$]	R1 = 0.0161, wR2 = 0.0382	R1 = 0.0192, wR2 = 0.0475	R1 = 0.0223, wR2 = 0.0504	R1 = 0.0250, wR2 = 0.0575
R indices (all data)	R1 = 0.0174, wR2 = 0.0387	R1 = 0.0207, wR2 = 0.0480	R1 = 0.0283, wR2 = 0.0519	R1 = 0.0260, wR2 = 0.0579

Eu(EtBTP)(NO$_3$)$_3$(H$_2$O)]·CH$_3$CN (3). To a stirred solution of Eu(NO$_3$)$_3$·5H$_2$O (0.05 mmol) in acetonitrile (3 mL) was added dropwise a solution of EtBTP (0.05 mmol) in acetonitrile (3 mL). The solution was stirred for 30 min and filtered. Crystals suitable for X-ray crystallography were obtained after slow evaporation of the solvent for several days. Calcd for EuC$_{21}$H$_{28}$N$_{11}$O$_{16}$: C, 33.79; H, 3.78; N, 20.64. Found: C, 33.65; H, 3.71; N, 20.75.

Crystal Structure Determinations. Structures were determined using a Bruker APEXII single-crystal diffractometer. An appropriate crystal was selected under paratone oil on a polarizing microscope and attached to a Kapton mount. A full sphere of data was collected with the sample cooled to 100 K using an Oxford nitrogen cryostream. An absorption correction utilized *SADABS*, the structure solution was performed using a β version of *SHELXT*, and refinement was carried out using a combination of *SHELX*[23] and *OLEX II.*[24] H atoms were added geometrically. A summary of the crystal data and structure refinement parameters are listed in Table 1. Detailed crystallographic tables and a CIF file are provided in the Supporting Information.

3. DENSITY FUNCTIONAL THEORY (DFT) CALCULATIONS

3.1. Crystal Structures. First-principles total energy calculations were performed using spin-polarized DFT, as implemented in the Vienna Ab initio Simulation Package.[25] The exchange-correlation energy was calculated using the generalized gradient approximation (GGA), with the para-metrization of Perdew, Burke, and Ernzerhof (PBE).[26] Pure functionals, such as the PBE or the Perdew−Wang[27] functionals, were found in previous studies to correctly describe the geometric parameters and properties of various lanthanide-containing structures observed experimentally.[28]

The interaction between the valence electrons and ionic cores was described by the projector-augmented-wave (PAW) method.[29,30] For trivalent Eu ions, 4f^6 electrons were treated explicitly as valence electrons in the Kohn−Sham (KS) equations and the remaining core electrons together with the nuclei were represented by PAW pseudopotentials. The KS equations were solved using the special blocked Davidson iterative matrix diagonalization scheme.[31] The plane-wave cutoff energy for the electronic wave functions was set to a value of 500 eV, ensuring the total energy of the system to be converged to within 1 meV/atom. Partial occupancies were set for each wave function using the tetrahedron method with Blöchl corrections.[32]

Ionic relaxation was carried out using the conjugate-gradient algorithm, and the Hellmann−Feynman forces acting on atoms were calculated with a convergence tolerance set to 0.01 eV/Å. A periodic unit cell approach was used in the calculations. In structural relaxation calculations, the structures determined from XRD were used as the starting geometries; structural relaxation was performed without symmetry constraints. The Brillouin zone was sampled using the Monkhorst−Pack k-point scheme[33] with k-point meshes of $3 \times 3 \times 3$ for structures **1, 2a**, and **2b** and $3 \times 3 \times 1$ for structure **3**.

3.2. Structures of Molecular Complexes. All-electron scalar relativistic calculations of the optimized geometries of molecular complexes with Eu and Am metal centers and RBTP ligands (R = H, Me, Et) were performed using DFT as implemented in the *DMol3* software.[34] The exchange-correlation energy was calculated using GGA, with the PBE

Table 2. Complexes Detected by ESI-MS for a 10^{-3} M Ligand with Varying $Eu(NO_3)_3$ Concentration with a Total Metal-to-Ligand Ratio of 0.1−10 in the Acetonitrile Medium in the Absence of TMAN

Ln³⁺	complex	HBTP		MeBTP		EtBTP	
		species	m/z	species	m/z	species	m/z
La³⁺	LnL			$[LaL(NO_3)(S)_4]^{2+}$	328.9	$[LaL(NO_3)(S)_4]^{2+}$	357.1
				$[LaL(NO_3)_2(S)]^+$	596.5	$[LaL(NO_3)_2(S)]^+$	652.7
				$[LaL(NO_3)_2(S)_2]^+$	637.4	$[LaL(NO_3)_2(S)_2]^+$	693.7
	LnL₂	$[LaL_2(NO_3)_2]^+$	736.5	$[LaL_2(NO_3)(S)]^{2+}$	414.1	$[LaL_2(NO_3)(S)]^{2+}$	470.1
				$[LaL_2(NO_3)_2]^+$	848.9	$[LaL_2(NO_3)_2]^+$	959.6
	LnL₃						
Eu³⁺	LnL			$[EuL(NO_3)_2(S)]^+$	608.0	$[EuL(NO_3)_2(S)]^+$	666.7
	LnL₂	$[EuL_2(NO_3)_2]^+$	748.6	$[EuL_2(NO_3)(S)]^{2+}$	421.3	$[EuL_2(NO_3)(S)]^{2+}$	476.7
				$[EuL_2(NO_3)_2]^+$	861.2	$[EuL_2(NO_3)_2]^+$	975.1
				$[EuL_2]^{2+}$	369.6		
	LnL₃	$[EuL_3(NO_3)]^{2+}$	462.7	$[EuL_3]^{3+}$	343.9	$[EuL_3]^{3+}$	400.0
				$[EuL_3(NO_3)]^{2+}$	546.9	$[EuL_3(NO_3)]^{2+}$	630.8
				$[EuL_3(H)_{-1}]^{2+}$	515.3	$[EuL_3(H)_{-1}]^{2+}$	599.3
Er³⁺	LnL	$[ErL(NO_3)_2(S)]^+$	567.7	$[ErL(NO_3)_2(S)]^+$	625.7	$[ErL(NO_3)_2(S)]^+$	679.7
		$[ErL(NO_3)(S)_3]^{2+}$	295.1				
	LnL₂	$[ErL_2(NO_3)_2]^+$	763.7	$[ErL_2(NO_3)(S)]^{2+}$	428.4	$ErL_2(NO_3)(S)]^{2+}$	484.1
		$[ErL_2(NO_3)(S)]^{2+}$	371.7	$[EuL_2]^{2+}$	377.1	$[ErL_2(NO_3)_2]^+$	989.9
	LnL₃	$[ErL_3(NO_3)]^{2+}$	469.7	$[ErL_3]^{3+}$	348.8	$[ErL_3]^{3+}$	404.9
				$[ErL_3(NO_3)]^{2+}$	554.3	$[ErL_3(NO_3)]^{2+}$	638.3
				$[ErL_3(H)_{-1}]^{2+}$	521.8	$[ErL_3(H)_{-1}]^{2+}$	606.2

Table 3. Complexes Detected by ESI-MS for a 10^{-3} M Ligand with Varying $Eu(NO_3)_3$ Concentration with a Total Metal-to-Ligand Ratio of 0.1−10 in the Acetonitrile Medium in the Presence of 0.01 M TMAN

Ln³⁺	complex	HBTP		MeBTP		EtBTP	
		species	m/z	species	m/z	species	m/z
La³⁺	LnL	$[LaL(NO_3)_2(S)]^+$	540.3	$[LaL(NO_3)_2]^+$	556.4	$[LaL(NO_3)_2]^+$	612.3
	LnL₂			$[LaL_2(NO_3)_2]^+$	849.2	$[LaL_2(NO_3)_2]^+$	961.4
	LnL₃						
Eu³⁺	LnL	$[EuL(NO_3)_2(S)]^+$	553.1	$[EuL(NO_3)_2]^+$	569.3	$[EuL(NO_3)_2]^+$	625.1
		$[EuL(NO_3)_2]^+$	513.1				
	LnL₂			$[EuL_2(NO_3)_2]^+$	861.3	$[EuL_2(NO_3)_2]^+$	975.7
	LnL₃						
Er³⁺	LnL	$[ErL(NO_3)_2(S)]^+$	568.3	$[ErL(NO_3)_2]^+$	588.1	$[ErL(NO_3)_2]^+$	638.7
	LnL₂			$[ErL_2(NO_3)_2]^+$	877.3	$[ErL_2(NO_3)_2]^+$	990.9
	LnL₃					$[ErL_3]^{3+}$	405.1
						$[ErL_3(NO_3)]^{2+}$	638.3
						$[ErL_3(H)_{-1}]^{2+}$	605.9

parametrization. Double numerical basis sets including polarization functions on all atoms (DNP) were used in the calculations. The DNP basis set corresponds to a double-ζ quality basis set with a p-type polarization function added to H atoms and d-type polarization functions added to heavier atoms.[34] In the generation of the numerical basis sets, a global orbital cutoff of 5.9 Å was used. The energy tolerance in the self-consistent-field calculations was set to 10^{-6} hartree. Optimized geometries were obtained without symmetry constraints using the direct inversion in a subspace method (DIIS) with an energy convergence tolerance of 10^{-5} hartree and a gradient convergence of 2×10^{-3} hartree/bohr. The charge density was expressed by a nucleus-centered multipole expansion truncated at the octupole level. The spin−orbit coupling was neglected in the calculations because it is expected to be small in a strong ligand field.

4. RESULTS AND DISCUSSION

4.1. ESI-MS. ESI-MS studies were performed on the lanthanide (La^{3+}, Eu^{3+}, and Er^{3+}) complexes of HBTP, MeBTP, and EtBTP in the acetonitrile medium by varying the metal-to-ligand ratio from 0.1 to 10. In order to see the effect of the nitrate ion, these experiments were carried out in the absence and presence of 0.01 M TMAN. All of the metal−ligand complexes identified in the absence and presence of 0.01 M TMAN from the ESI-MS spectra are listed in Tables 2 and 3, respectively. ESI-MS spectra of Eu^{3+} complexes of the three RBTP ligands and La^{3+} and Er^{3+} complexes of EtBTP with a ligand-to-metal ratio of 1:1 in the absence of TMAN are shown in Figures 6 and 7, respectively. In the following sections for the lanthanide (Ln^{3+}) complexes, RBTP ligands are written as L and the solvent acetonitrile molecules are represented as S.

In the Absence of TMAN. All three lanthanides (La^{3+}, Eu^{3+}, and Er^{3+}) mainly form a 1:2 complex of the type $[LnL_2(NO_3)_2]^+$ with HBTP, as observed from ESI-MS peaks with values of m/z 736.5, 748.6, and 763.7, respectively (Table
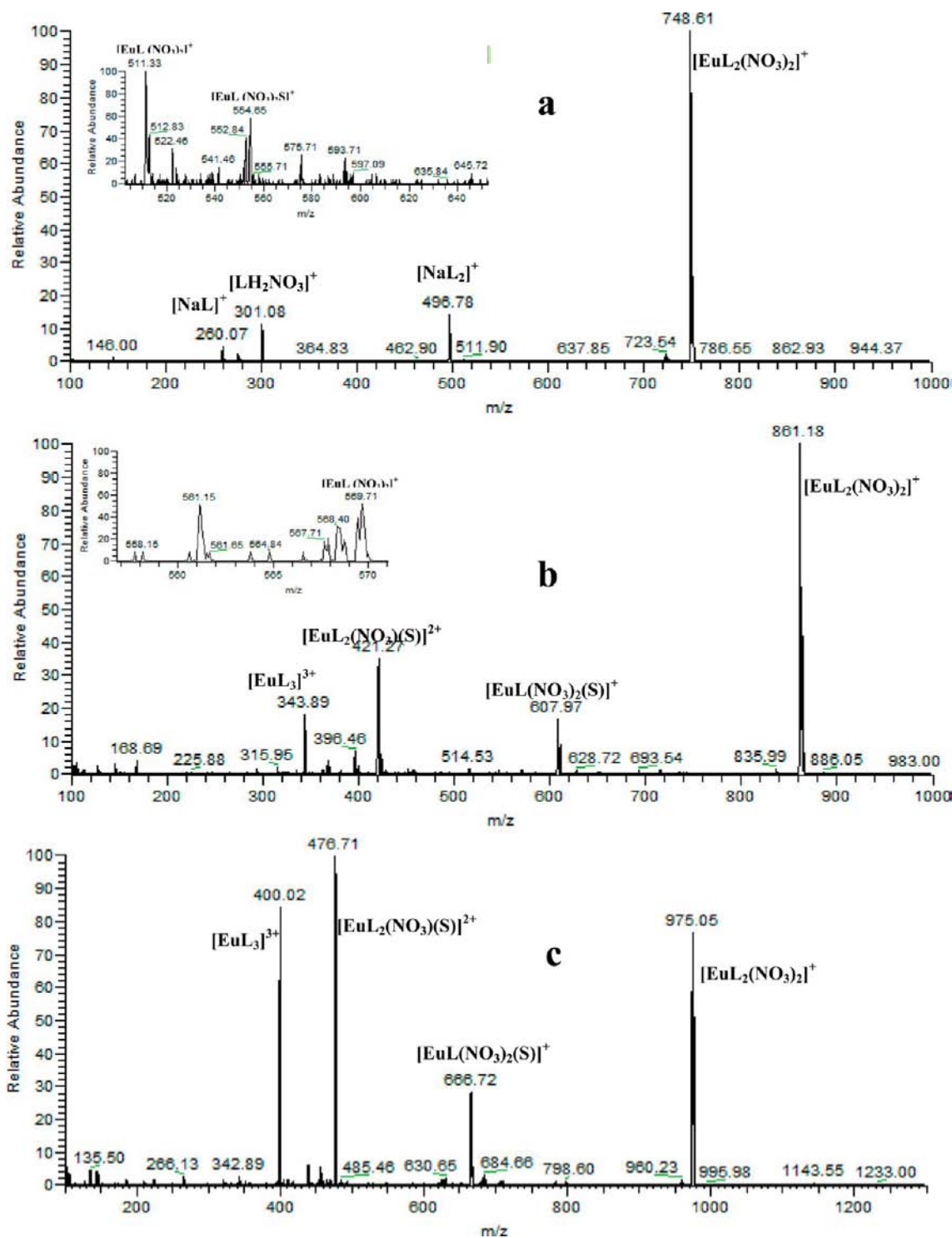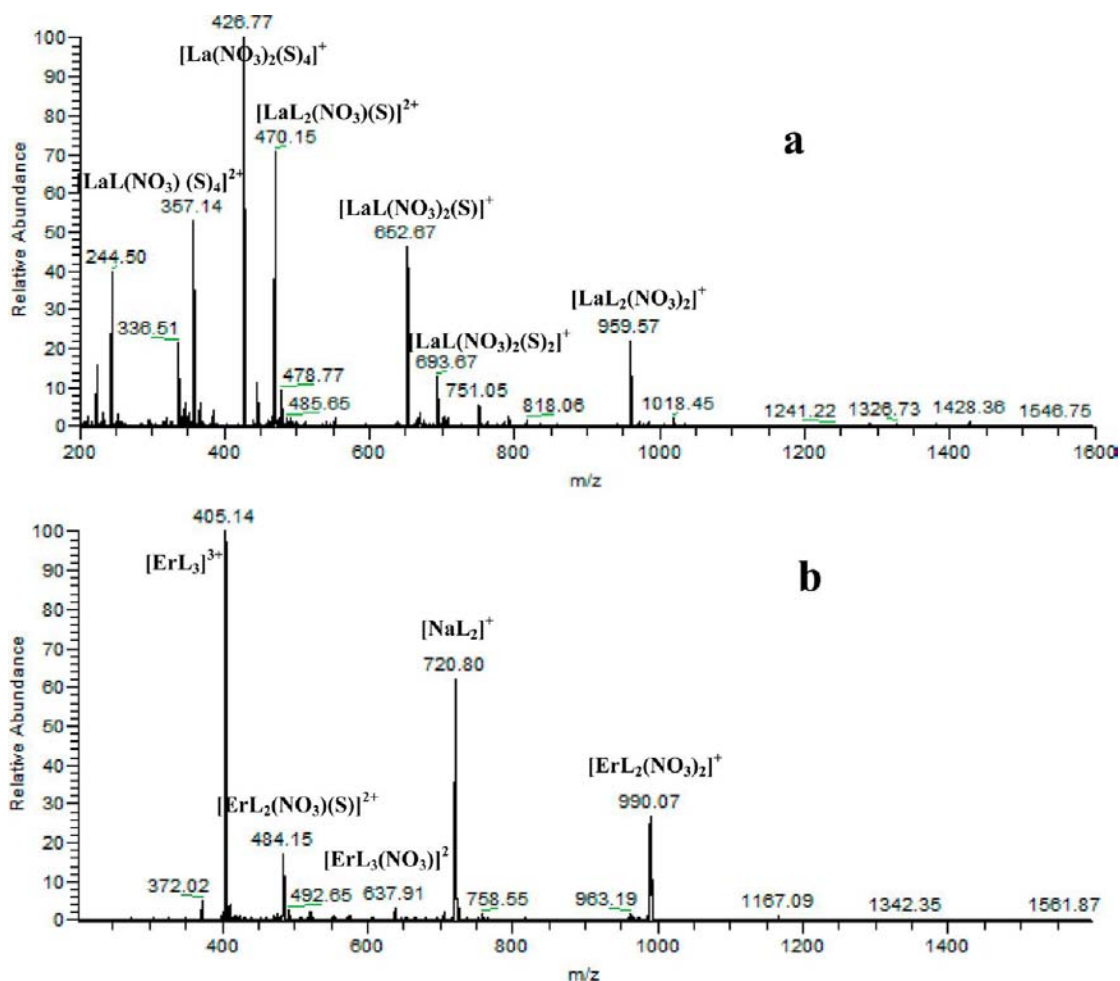
Figure 6. ESI-MS spectra of Eu^{3+} complexes of BTP derivatives (a, HBTP; b, MeBTP; c, EtBTP) in acetonitrile in the absence of TMAN with a metal-to-ligand ratio of 1:1.

2). This observation supports the formation of 12-coordinated lanthanide complexes of the type $LnL_2(NO_3)_3$ with HBTP in the solid phase.[9] No other species is detected for La^{3+}, whereas small peaks at values of m/z 462.7 and 469.7 correspond to the 1:3 complex $[LnL_3(NO_3)]^{2+}$ for Eu^{3+} and Er^{3+}, respectively. Apart from this, Er^{3+} forms 1:1 complexes of the types $[ErL(NO_3)_2(S)]^+$ and $[ErL(NO_3)(S)_3]^{2+}$ at m/z 567.7 and 295.1, respectively. The number of species identified was higher for the complexes of MeBTP and EtBTP. La^{3+} forms 1:1 and

1:2 complexes with both ligands. Tetra- and disolvated 1:1 La^{3+} complexes ($[LaL(NO_3)(S)_4]^{2+}$ and $[LaL(NO_3)_2(S)_2]^+$) were detected, which were not observed in the case of heavier lanthanides Eu^{3+} and Er^{3+}. The absence of higher solvated species for heavier lanthanides is probably due to their smaller size, which restricts their coordination number. A mono-solvated 1:1 complex of the type $[LnL(NO_3)_2(S)]^+$ with lower coordination number was, however, present for all three lanthanides. The presence of such a solvation shell shows soft

Figure 7. ESI-MS spectra of La^{3+} and Er^{3+} complexes of EtBTP derivatives (a, La^{3+}-EtBTP; b, Er^{3+}-EtBTP) in acetonitrile in the absence of TMAN with a metal-to-ligand ratio of 1:1.

(low-declustering) conditions of the ionization and measurement processes.[35] $[LnL_2(NO_3)(S)]^{2+}$ and $[LnL_2(NO_3)_2]^+$ were observed as 1:2 complexes in the case of all three lanthanides with both MeBTP and EtBTP ligands. La^{3+} does not form any 1:3 complex with any of the ligands studied, whereas both Eu^{3+} and Er^{3+} form a 1:3 complex, $[LnL_3]^{3+}$, with both ligands (MeBTP and EtBTP). This $[LnL_3]^{3+}$ type of species was, however, not at all observed in the case of HBTP with any of the lanthanides studied. For a particular lanthanide ion (Eu^{3+} or Er^{3+}), the relative intensity of the $[LnL_3]^{3+}$ species was higher in the case of EtBTP compared to that of MeBTP (Figure 6 for Eu^{3+}). This indicates that the increase in the hydrophobic alkyl chain length favors formation of the $[LnL_3]^{3+}$ species. If we consider a particular ligand (MeBTP or EtBTP), the intensity for $[LnL_3]^{3+}$ species relative to other lower stoichiometric species was higher in the case of Er^{3+} compared to Eu^{3+} (Figure 6c vs Figure 7b for EtBTP), indicating the higher tendency to form $[LnL_3]^{3+}$ species in the case of heavier lanthanides. Colette et al. have also shown a monotonic increase in the conditional stability constants for formation of the $[LnL_3]^{3+}$ species with 5,6-diisopropylbis(1,2,4-triazin-3-yl)pyridine (iPrBTP) as we go along the lanthanide series.[36] This was attributed to the electrostatic nature of the metal−ligand interaction in those complexes. Another two types of 1:3 complexes, $[LnL_3(NO_3)]^{2+}$ and $[LnL_3(H)_-]^{2+}$, were observed in the case of Eu^{3+} and Er^{3+} with both MeBTP and EtBTP.

Similar species were also reported with different alkyl BTP derivatives in a water/methanol mixture.[13] They confirmed formation of the $[LnL_3(H)_{-1}]^{2+}$ species through HNO_3 release of the $[LnL_3(NO_3)]^{2+}$ complex using MS/MS spectra. Similar to the observation of Colette et al.,[13] the formation of a small amount of charge reduced ions $[LnL_2]^{2+}$ was observed in the case of MeBTP complexes of Eu^{3+} and Er^{3+}, which was suggested as a result of the fragmentation pathway of other complex species. EtBTP, however, did not form a similar charge-reduced ion with any of the lanthanides studied.

In the Presence of 0.01 M TMAN. The speciation was completely different in the presence of 0.01 M TMAN (Table 3). HBTP was found to form a 1:1 complex only with all three lanthanides studied, and no 1:2 complex was detected here. A monosolvated 1:1 species, $[LnL(NO_3)_2(S)]^+$, was observed in the case of all three lanthanides. Besides this, a small peak at m/z 513.1 was detected for the Eu^{3+} complex of HBTP corresponding to the species $[EuL(NO_3)_2]^+$ and a similar species was not observed in the case of La^{3+} and Er^{3+}. Both 1:1 ($[LnL(NO_3)_2]^+$) and 1:2 ($[LnL_2(NO_3)_2]^+$) complexes were, however, formed for all three lanthanides with MeBTP and EtBTP. A general observation here is that population of solvated species is much lower in the presence of 0.01 M TMAN, which is due to the incapability of the acetonitrile molecule to compete with the strongly complexing nitrate ions. Unlike the observation in the absence of TMAN, MeBTP does

not form any 1:3 complex with any of the lanthanides studied. This is because of the strong competition from the nitrate ions, which prevents the formation of higher stoichiometric complexes. EtBTP, however, forms a 1:3 complex with only Er^{3+}. We have already discussed that formation of a 1:3 complex is most favored with the heavier lanthanide, Er^{3+}, and most hydrophobic, EtBTP, among all of the systems considered in the present work. A 1:3 complex of Er^{3+} and EtBTP is, therefore, observed even in the presence of excess nitrate ion (0.01 M TMAN) in the medium.

4.2. TRLFS Study. *In the Absence of TMAN.* The emission spectra of $Eu(NO_3)_3$ and its complexes with HBTP, MeBTP, and EtBTP in acetonitrile in the absence of TMAN are shown in Figure 8. Compared to $Eu(NO_3)_3$, coordination with the
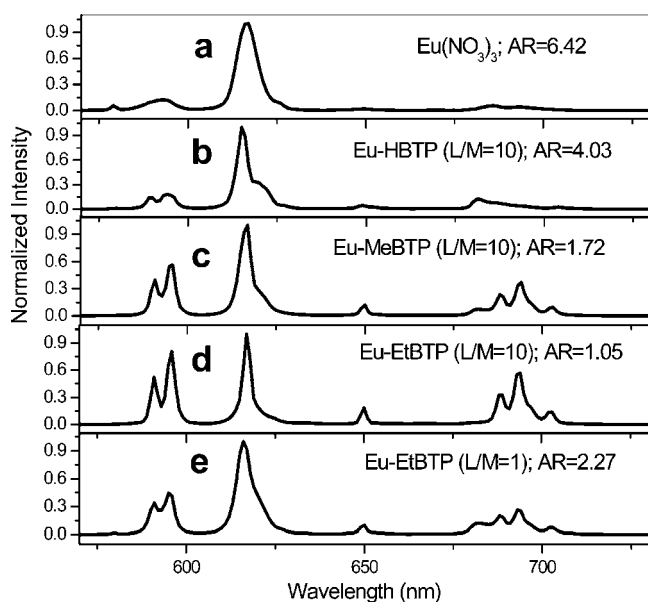
Figure 8. Emission spectra of $Eu(NO_3)_3$ and its complex ([L]/[M] = 10) in acetonitrile in the absence of TMAN.

RBTP ligands causes distinct splitting of the $^5D_0 \rightarrow ^7F_1$ emission band at 585−600 nm. The $^5D_0 \rightarrow ^7F_2$ transition at 610−625 nm is hypersensitive and changes in the ligand field of Eu^{III}, which is reflected by changes of the transition ratio ($^7F_2/^7F_1$), known as the asymmetry ratio. $Eu(NO_3)_3$ displays a transition ratio $^7F_2/^7F_1 = 6.42$, which decreases upon complexation with RBTP ligands. In the case of the EtBTP complex (Figure 8d), the ratio decreases to 1.05 at a ligand-to-metal ratio ([L]/[M]) = 10. This $^7F_2/^7F_1$ transition ratio value and splitting pattern of the emission spectra (double of the $^5D_0 \rightarrow ^7F_1$ transition at 585−600 nm and triple of the $^5D_0 \rightarrow ^7F_4$ transition at 680−710 nm) are the signatures of the D_3-symmetric species $[EuL_3]^{3+}$.[14,17] The lifetime (τ) value of this $[EuL_3]^{3+}$ species was observed as 2061 ± 16 μs (Table 4). The lifetime value, however, cannot be the signature of the species because it may vary significantly depending on the solvent medium and nature of the ligand. The same $[EuL_3]^{3+}$ species of nPrBTP shows the lifetime values of 1727[15] and 2437 μs[18] in methanol/water (1:1) and TPH/octanol (7:3) mixtures, respectively, whereas a similar iPrBTP complex shows a lifetime value as high as 2700 μs even in a methanol/water (1:1) mixture.[14] The emission spectrum of the Eu^{III}-EtBTP complex was significantly altered by changing the ligand-to-metal ratio to 1 (Figure 8e). The transition ratio ($^7F_2/^7F_1$) value of 2.27 and

Table 4. Lifetime Data of Europium(III) Complexes of BTP Ligands in the Acetonitrile Medium ([L]/[M] = 50)[a]

| complex | with TMAN | | without TMAN | |
	τ	species responsible	τ	species responsible
$Eu(NO_3)_3$	476 ± 23		350 ± 2	
Eu^{III}-HBTP	557 ± 13	LnL	1125 ± 56	LnL_2
Eu^{III}-MeBTP	1617 ± 14	LnL_2	1812 ± 23	LnL_3
Eu^{III}-EtBTP	1744 ± 17	LnL_2	2061 ± 16	LnL_3

[a]The ionic strength was maintained by 0.01 M TMAN.

the quadruple splitting of the $^5D_0 \rightarrow ^7F_4$ transition at 680−710 nm says that the spectrum is not solely due to the 1:3 complex $[EuL_3]^{3+}$. Some other lower stoichiometric complexes with lower symmetry, therefore, must have appeared. The ESI-MS study also supports this observation by showing the presence of various 1:2 and 1:1 complexes. In the case of the Eu-HBTP complex, no signature of the $[EuL_3]^{3+}$ type of species was observed. Figure 8b shows the transition ratio ($^7F_2/^7F_1$) value of 4.03, which can be attributed to the 1:2 Eu^{3+} complex of HBTP, as observed from the ESI-MS study, and the lifetime of this complex was 1125 ± 56 μs (Table 4 and Figure 11). We must remember here that ESI-MS spectra of the Eu-HBTP complex also show the absence of the $[EuL_3]^{3+}$ type of species even in the presence of excess ligand. Eu-MeBTP, however, shows intermediate behavior. Unlike the EtBTP complex, the emission spectrum of the MeBTP complex at [L]/[M] = 10 (Figure 8c) also is not solely due to the $[LnL_3]^{3+}$ species, and it has a close resemblance to the emission spectrum of the Eu-EtBTP complex with a lower [L]/[M] value (Figure 8e). The ESI-MS study of this Eu-MeBTP complex also shows the formation of a lower stoichiometric complex in significant proportion compared to the symmetric species $[LnL_3]^{3+}$. A characteristic emission spectrum of the $[EuL_3]^{3+}$ type of species for the MeBTP complex was observed at [L]/[M] = 50, and the lifetime of this species was found to be 1812 ± 23 μs (Table 4 and Figure 11).

In the Presence of 0.01 M TMAN. The emission spectra (Figure 9) do not show formation of the $[EuL_3]^{3+}$ type of species with any of the three RBTP ligands studied in the acetonitrile medium in the presence of 0.01 M TMAN. Moreover, the spectra of the MeBTP (Figure 9c) and EtBTP (Figure 9d) complexes in the presence of 0.01 M TMAN are quite similar to the emission spectrum of the Eu-HBTP complex in the absence of TMAN (Figure 8b). This indicates that a 1:2 complex similar to that formed in the case of HBTP in the absence of TMAN is responsible for the emission spectra of the MeBTP and EtBTP complexes in the presence of 0.01 M TMAN. As we discussed in section 4.1, the ESI-MS study also shows that the $[EuL_3]^{3+}$ type of species is not formed in the presence of 0.01 M TMAN in the case of any of these three ligands. The 1:2 complex of the type $[LnL_2(NO_3)_2]^+$ (as observed in the case of HBTP complexes in the absence of TMAN) is the highest stoichiometric complex observed for MeBTP and EtBTP in the presence of 0.01 M TMAN, and the lifetimes of these complexes were found to be 1617 ± 14 and 1744 ± 17 μs, respectively (Table 4 and Figure 12). The Eu^{3+} complex of HBTP in the presence of 0.01 M TMAN, however, is much different with a splitting in the hypersensitive $^5D_0 \rightarrow ^7F_2$ transition peak at 610−625 nm and a very high transition ratio ($^7F_2/^7F_1$) value of 6.80 (Figure 9b), which cannot be attributed to the 1:2 complex, as observed in the absence of
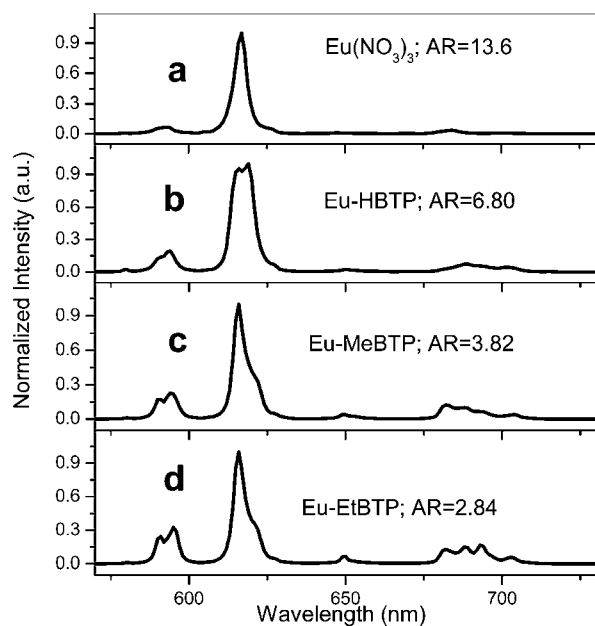
**Figure 9.** Emission spectra of $Eu(NO_3)_3$ and its complex ([L]/[M] = 10) in acetonitrile in the presence of 0.01 M TMAN.

TMAN. This emission spectrum can be attributed to a 1:1 complex with a lifetime of 553 ± 13 μs (Table 4 and Figure 12), as was also observed from the ESI-MS study (section 4.1). Literature reports show formation of the $[EuL_3]^{3+}$ type of species with EtBTP[37] and nPrBTP[38] in the methanol medium even in the presence of 0.01 M tetrapropylammonium nitrate and tetraethylammonium nitrate, respectively. It will, therefore, be of interest to study the complexes of all three ligands in the methanol medium in the presence of 0.01 M TMAN for comparison. Emission spectra of $Eu(NO_3)_3$ and its complexes with RBTP ligands in the methanol medium in the presence of 0.01 M TMAN (Figure 10) show that HBTP is incapable of
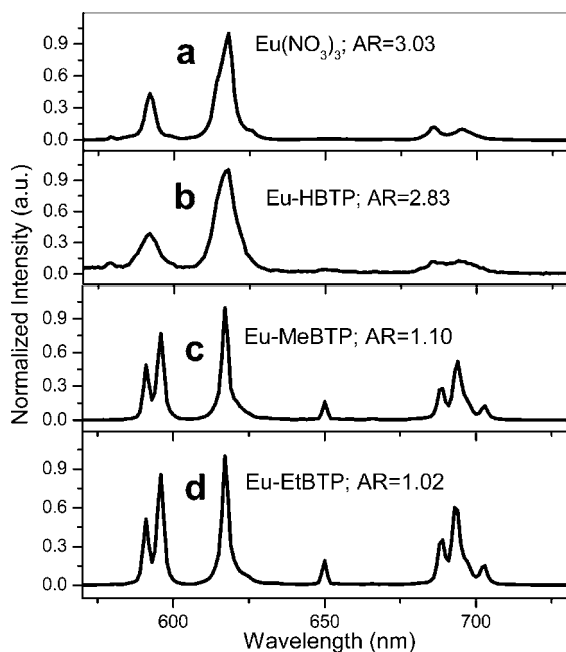
Figure 10. Emission spectra of $Eu(NO_3)_3$ and its complex ([L]/[M] = 10) in methanol in the presence of 0.01 M TMAN.
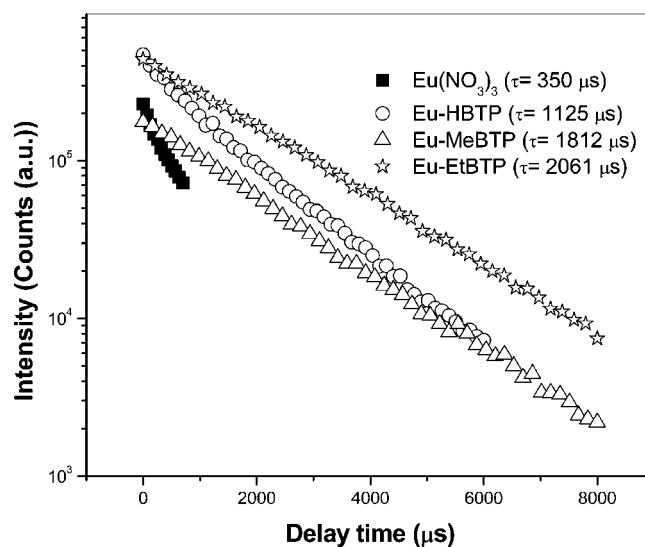
Figure 11. Decay of the fluorescence intensity of the $^5D_0 \rightarrow {}^7F_2$ transition peak of $Eu(NO_3)_3$ and its complexes with different BTP ligands with a metal-to-ligand ratio of 1:50 in the acetonitrile medium in the absence of TMAN (τ values shown here are the average values considering the decay of other peaks also).
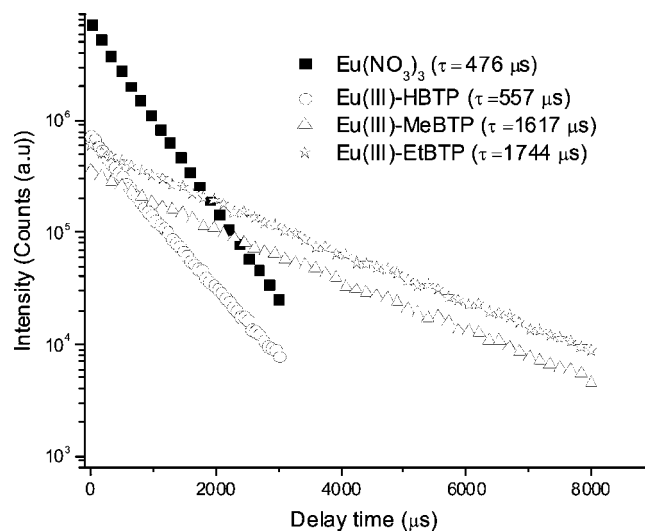
Figure 12. Decay of the fluorescence intensity of the $^5D_0 \rightarrow {}^7F_2$ transition peak of $Eu(NO_3)_3$ and its complexes with different BTP ligands with a metal-to-ligand ratio of 1:50 in the acetonitrile medium in the presence of 0.01 M TMAN (τ values shown here are the average values considering the decay of other peaks also).

forming any complex in this condition because the emission spectrum is very similar to that of $Eu(NO_3)_3$ and no change in the UV−vis absorption spectrum of HBTP was observed with the addition of $Eu(NO_3)_3$ in a methanol medium. MeBTP and EtBTP, however, form a 1:3 complex of the type $[EuL_3]^{3+}$ in the methanol medium even in the presence of 0.01 M TMAN. This difference in the complexation behavior of these two ligands in acetonitrile and methanol media can be attributed to the difference in the solvation efficiency of these two solvents. Lanthanide ions are hard cations, and therefore how strongly a solvent can solvate these cations is expressed as the hard donor strength (HD_s) of the particular solvent.[39] The HD_s value is much lower for acetonitrile (9.9) compared to methanol (16.7), resulting in much lower solvation of the lanthanide ions in the

acetonitrile medium compared to the methanol medium. Nitrate ions can, therefore, form a stronger inner-sphere complex with the lanthanide ions in the acetonitrile medium. Stronger nitrate complexation of Eu^{3+} in the acetonitrile medium compared to that in the methanol medium was also shown by fluorescence spectroscopy, indicating the presence of the Eu^{3+} ion as a nitrate complex in the acetonitrile medium.[40] This causes much difficulty in the formation of the $[LnL_3]^{3+}$ type of species, where all nitrate ions are to be removed completely from the inner sphere, and this became impossible here in the presence of excess nitrate ion in the acetonitrile medium.

4.3. UV–Vis Spectrophotometric Study. UV–vis spectrophotometric titrations were carried out in order to determine the stability constants of Am^{3+} and different lanthanide ions with the RBTP ligands in the acetonitrile medium at 0.01 M fixed ionic strength maintained using TMAN. Consistent with the ESI-MS and TRLFS results, only a 1:1 complex was observed with HBTP in the case of all lanthanides studied, whereas in the case of MeBTP and EtBTP, higher stoichiometric complexes were formed, and their stability constant values are listed in Table 5. Am^{3+}, however,

Table 5. Species Observed and Complexation Constants of Various Lanthanide and Americium Nitrate Complexes with Different BTP Ligands in the Acetonitrile Medium in the Presence of 0.01 M TMAN Calculated from the UV–Vis Spectrophotometric Titrations

M^{3+}		HBTP	MeBTP	EtBTP
La^{3+}	LnL	$\log \beta_{11} = 3.43 \pm 0.01$	$\log \beta_{11} = 4.11 \pm 0.01$	$\log \beta_{11} = 4.41 \pm 0.01$
Nd^{3+}	LnL	$\log \beta_{11} = 3.62 \pm 0.02$	$\log \beta_{11} = 4.86 \pm 0.01$	$\log \beta_{11} = 4.84 \pm 0.01$
	LnL$_2$		$\log \beta_{12} = 7.51 \pm 0.01$	$\log \beta_{12} = 9.50 \pm 0.01$
Eu^{3+}	LnL	$\log \beta_{11} = 3.43 \pm 0.02$	$\log \beta_{11} = 4.47 \pm 0.01$	$\log \beta_{11} = 4.88 \pm 0.01$
	LnL$_2$		$\log \beta_{12} = 8.58 \pm 0.03$	$\log \beta_{12} = 10.21 \pm 0.03$
Tb^{3+}	LnL	$\log \beta_{11} = 3.47 \pm 0.03$	$\log \beta_{11} = 4.15 \pm 0.02$	$\log \beta_{11} = 5.13 \pm 0.05$
	LnL$_2$		$\log \beta_{12} = 8.84 \pm 0.01$	$\log \beta_{12} = 10.38 \pm 0.04$
	LnL$_3$			$\log \beta_{13} = 14.62 \pm 0.08$
Er^{3+}	LnL	$\log \beta_{11} = 3.35 \pm 0.02$	$\log \beta_{11} = 4.20 \pm 0.02$	$\log \beta_{11} = 5.66 \pm 0.05$
	LnL$_2$		$\log \beta_{12} = 8.92 \pm 0.01$	$\log \beta_{12} = 11.11 \pm 0.06$
	LnL$_3$			$\log \beta_{13} = 16.09 \pm 0.07$
Am^{3+}	AmL	$\log \beta_{11} = 4.32 \pm 0.22$		
	AmL$_2$	$\log \beta_{12} = 6.92 \pm 0.45$	$\log \beta_{12} = 9.96 \pm 0.20$	$\log \beta_{12} = 12.62 \pm 0.28$
	AmL$_3$			$\log \beta_{13} = 16.09 \pm 0.01$

forms both 1:1 and 1:2 complexes with HBTP with higher stability constants compared to the lanthanides, which indicates more affinity of these classes of ligands toward trivalent actinides. The stability constant values presented here are much higher compared to the literature values reported in a methanol/water mixture.[11,41] The reason for the lower stability constants in a methanol/water mixture is due to the higher desolvation energy requirement prior to complexation in this

stronger solvating medium. On the other hand, the desolvation energy requirement in the acetonitrile medium must be much lower because of the poor solvation power of acetonitrile toward the hard lanthanide ions, as described in section 4.2. For the same reason, the $\log \beta_{13}$ value for Eu^{3+} complexation with nPrBTP is 2 orders of magnitude lower in a methanol/water mixture[15] compared to that in a pure methanol medium.[38] From the $\log \beta_{11}$ values listed in Table 5, no regular trend was observed in HBTP complexation along the lanthanide series. This suggests that, besides the metal−ligand electrostatic interactions, other factors described by Ionova et al.[41] must be playing a significant role in controlling the complexation behavior of HBTP. Unlike other lanthanides studied, La^{3+} forms only a 1:1 complex even with MeBTP and EtBTP. Similarly, only a 1:1 La^{3+} complex was also reported with EtBTP[37] and nPrBTP[38] in the methanol medium. The ESI-MS study presented in section 4.1, however, shows the presence of a 1:2 complex of La^{3+} with MeBTP and EtBTP, which is not detected in a UV−vis spectrophotometric study probably because of its insignificant contribution to the UV−vis spectra. For the other lanthanides, however, 1:1 and 1:2 complexes have been observed for MeBTP and EtBTP, which is consistent with the ESI-MS results in the presence of 0.01 M TMAN. A 1:3 complex of EtBTP is found in the case of Tb^{3+} and Er^{3+}, which is also in line with the observation of a ESI-MS study in the presence of TMAN. Am^{3+} forms only a 1:2 complex with MeBTP, whereas it forms both 1:2 and 1:3 complexes with EtBTP. This indicates the tendency of Am^{3+} to form higher stoichiometric complexes with RBTP ligands compared to the Ln^{3+} ions. In the case of all three RBTP ligands, the stability constant values of Am^{3+} complexes are higher compared to those of the Ln^{3+} ions. Formation of the higher stoichiometric Am^{3+} complexes with higher stability constant values in spite of stronger nitrate complexation in a poor solvating acetonitrile medium is the reflection of a higher affinity of these ligands toward trivalent actinides compared to the lanthanides. The $\log \beta_{11}$ values increase in the order HBTP < MeBTP < EtBTP for all lanthanides studied. Similar increases in the stability constant values with increasing the alkyl chain length are also reported in the literature.[11,41]

4.4. Single-Crystal XRD Studies. Boucher et al.[9] observed the formation of 12-coordinated HBTP complexes of early lanthanides of bigger ionic size like Pr^{3+} and Nd^{3+} when they were prepared in the acetonitrile medium. No structural study is, however, reported on the HBTP complex of smaller size, heavier lanthanides. It will, therefore, be of interest to study the structures of HBTP complexes of a smaller lanthanide ion, viz., Eu^{3+}, where the coordination number of 12 is unlikely. It will also be interesting to compare the structures of Eu^{3+} complexes of MeBTP and EtBTP prepared in the same experimental conditions in order to understand the effect of the alkyl group on their complexation behavior in the solid state. The single-crystal XRD study shows different structures of Eu^{3+} complexes as we change the alkyl substituents. HBTP forms a dimeric Eu^{3+} complex (**1**) of the type $[Eu_2(HBTP)_2(NO_3)_6] \cdot 2CH_3CN$, where the two Eu^{3+} ions are bridged through the nitrate ions (Figure 13). EtBTP, on the other hand, forms a monomeric complex (**3**) of composition $[Eu(EtBTP)(NO_3)_3(H_2O)] \cdot CH_3CN$. Interestingly, MeBTP shows intermediate behavior, where two different types of crystals (**2a** and **2b**) were isolated, out of which one (**2a**) was isomorphous with the EtBTP complex (**3**) and the other one (**2b**) was isomorphous with the HBTP complex (**1**). The Eu−N bond
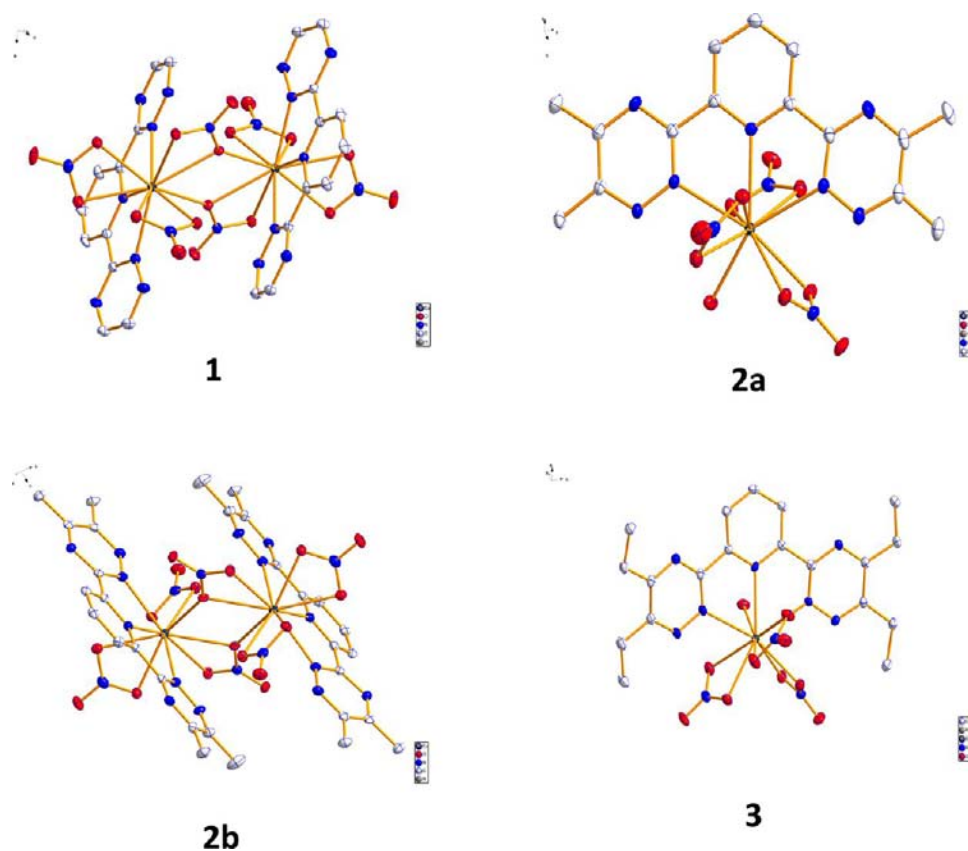
Figure 13. Structures of europium(III) complexes of RBTP (**1**, **2a**, **2b**, and **3**) prepared in the acetonitrile medium with ellipsoids at 50% probability. The H atoms and solvent molecules are omitted in the structures for clarity.

Table 6. Summary of the Eu^{III}-RBTP Crystal Data and Parameters Optimized with DFT

	europium(III) complex			
	1	**2a**	**2b**	**3**
formula	Eu$_2$(HBTP)$_2$(NO$_3$)$_6$·2CH$_3$CN	Eu(MeBTP)(NO$_3$)$_3$(H$_2$O)·CH$_3$CN	Eu$_2$(MeBTP)$_2$(NO$_3$)$_6$	Eu(EtBTP)(NO$_3$)$_3$(H$_2$O)·CH$_3$CN
cryst syst	triclinic	triclinic	monoclinic	triclinic
space group	$P\bar{1}$	$P\bar{1}$	$P2(1)/n$	$P\bar{1}$
unit cell dimens				
a (Å)	9.757	8.683	13.580	8.035
b (Å)	11.706	12.931	11.262	9.894
c (Å)	11.856	12.937	15.575	18.852
α (deg)	60.35	92.24	90	85.95
β (deg)	73.10	103.72	106.22	87.14
γ (deg)	72.11	107.70	90	84.84.
V (Å^3)	1104.44	1334.72	2287.20	1487.51
Z	1	2	2	2

distances in the isomorphous structures were compared, and with an increase in the alkyl groups, the Eu−N bond increases. Drew et al.[42] have also observed similar dimeric MeBTP complexes of Pr^{3+} and Nd^{3+} when they were prepared in the methanol medium, whereas EtBTP formed a monomeric complex. These observations reveal the fact that monomeric complexes are favored with the substituted BTP having a bigger alkyl chain. Very little correlation was observed between the solution- and solid-phase complexes. The 1:2 and 1:3 complexes, which were predominant from the solution-phase complexation studies, were not formed in the solid phase. However, after the ESI-MS spectra (Figure 6a,b) were carefully examined, the monomeric complexes [Eu(HBTP)(NO$_3$)$_2$]$^+$ (m/z 511.3) and [Eu(MeBTP)(NO$_3$)$_2$]$^+$ (m/z 569.7) were

observed, which may dimerize to form the solid-state dimeric complexes, whereas similar species were not observed in the case of EtBTP and no dimeric complexes were formed in the solid state either. The monomeric complex of the type [EuL(NO$_3$)$_2$(CH$_3$CN)]$^+$ was observed in the solution phase, where no water molecule was present. The monomeric complex formed in the solid state, however, contains one water molecule along with the acetonitrile medium. One thing was very clear from the ESI-MS spectra (Figure 6): that the relative abundance of the monomeric complex ([EuL-(NO$_3$)$_2$(CH$_3$CN)]$^+$) increased monotonously with increasing size of the alkyl group, which is consistent with the observation in the solid-phase complexes.
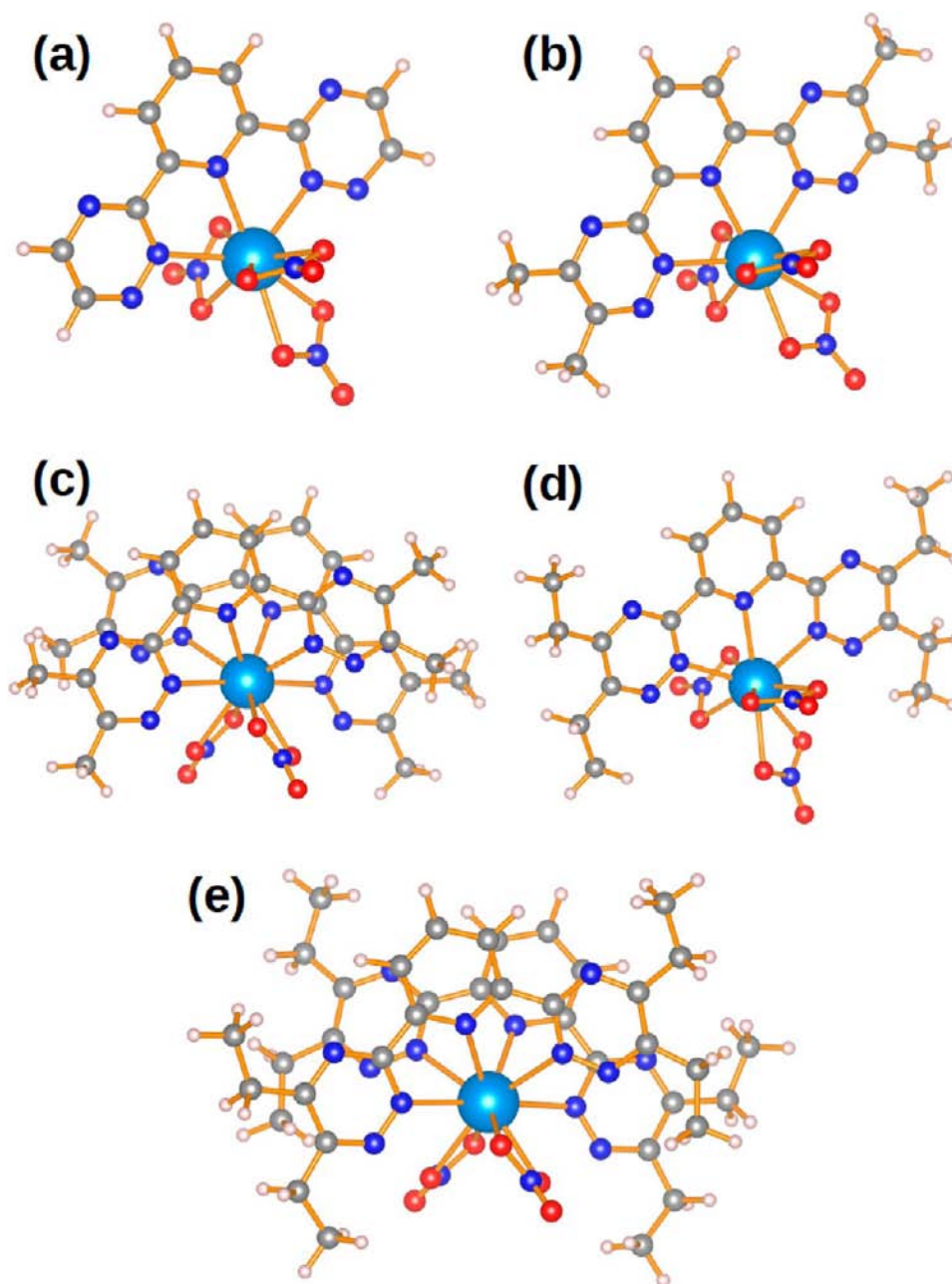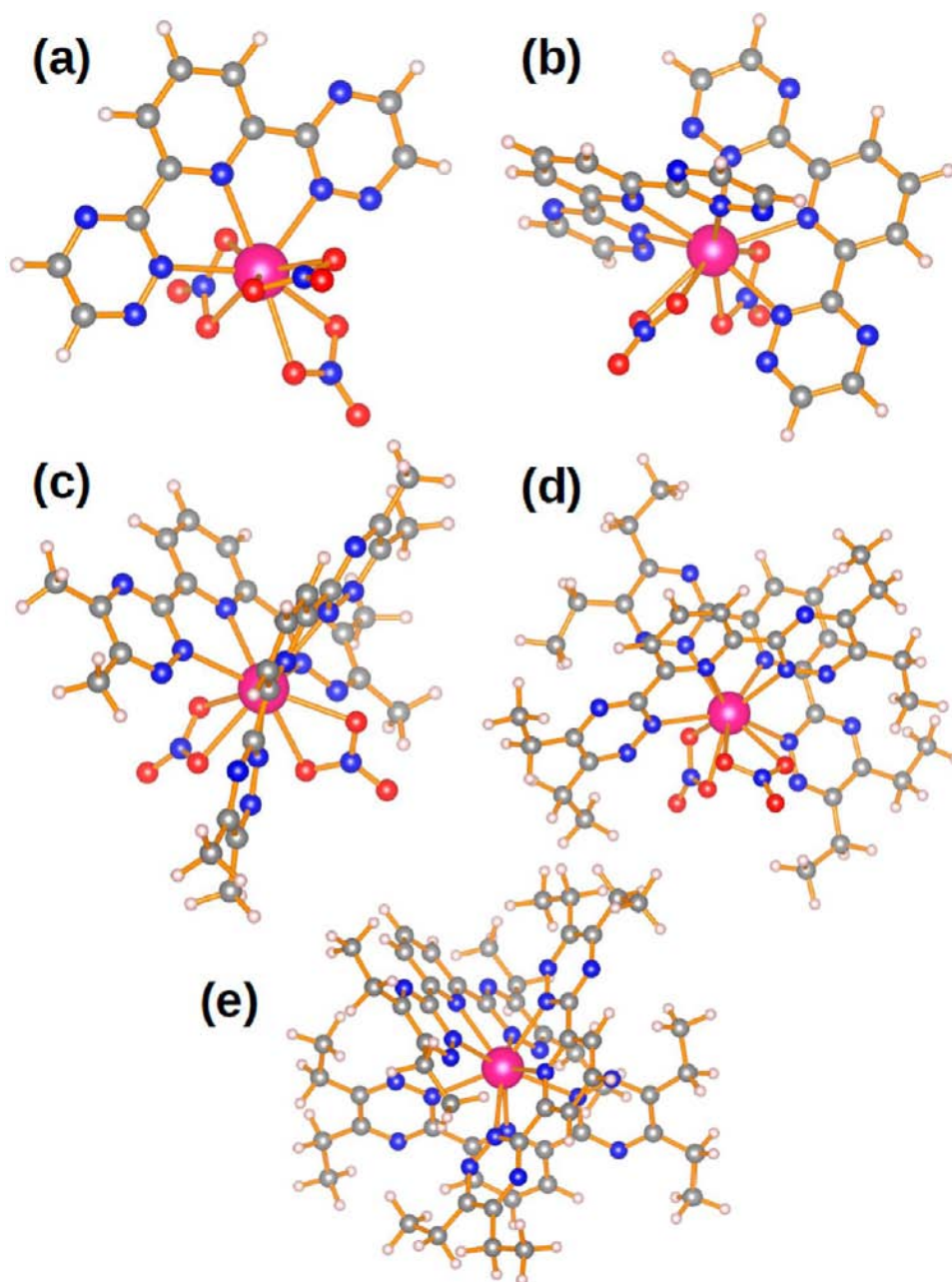
Figure 14. Equilibrium structures of Eu^{3+} complexes of RBTP (R = H, Me, Et) calculated using all-electron scalar relativistic DFT: (a) $Eu(HBTP)(NO_3)_3$, (b) $Eu(MeBTP)(NO_3)_3$, (c) $[Eu(MeBTP)_2(NO_3)_2]^+$, (d) $Eu(EtBTP)(NO_3)_3$, and (e) $[Eu(MeBTP)_2(NO_3)_2]^+$. Color legend: C, gray; Eu, cyan; H, white; N, blue; O, red.

4.5. DFT Studies. *Crystal Structures.* The structures of the crystals **1**, **2a**, **2b**, and **3** were relaxed with DFT starting from the geometries determined using XRD; the optimized crystal data and structural parameters are reported in Table 6. The computed structures are found to crystallize in space groups similar to those of the experimental structures, i.e., $P\bar{1}$ for **1**, **2a**, and **3** and $P2(1)/n$ for **2b**. As expected from standard GGA calculations, the calculated volumes consistently overestimate the experimental volumes, by 4.3% for **3**, 5.4% for **2a**, 7.8% for **1**, and 8.0% for **2b**; these results show that no particular treatment to account for strong electron correlation (e.g., GGA +U) is necessary for the present systems. The volume overestimation is systematically larger in crystal structures containing dimeric complexes (**1** and **2b**) than in structures with monomeric complexes (**2a** and **3**). Similar to experimental

findings, the average Eu−N bond distance increases with an increase in the size of the alkyl group: Eu−N = 2.561 Å in **1** with the HBTP ligand, Eu−N = 2.592 Å in **2a** and 2.579 Å in **2b** with the MeBTP ligand, and Eu−N = 2.607 Å in **3** with the EtBTP ligand; in the case of MeBTP, the average Eu−N distance is slightly more elongated for the monomeric complex than for the dimeric complex. The average Eu−O bond also shows a trend similar to that of the alkyl size; however, its variation is relatively limited: Eu−O = 2.527 Å in **1** (HBTP), Eu−O = 2.530 Å in **2a** and 2.532 Å in **2b** (MeBTP), and Eu−O = 2.539 Å in **3** (EtBTP). In the dimeric complexes, the Eu−O bond distances in the bridges are 2.566 and 2.586 Å in **1** and 2.553 and 2.632 Å in **2b**. In the monomeric complexes, the Eu−OH$_2$ bond distances are 2.414 Å in **2a** and 2.432 Å in **3**. Excluding the Eu−O bonds involved in the bridge of the

Figure 15. Equilibrium structures of Am^{3+} complexes of RBTP (R = H, Me, Et) calculated using all-electron scalar relativistic DFT: (a) $Am(HBTP)(NO_3)_3$, (b) $[Am(HBTP)_2(NO_3)_2]^+$, (c) $[Am(MeBTP)_2(NO_3)_2]^+$, (d) $[Am(EtBTP)_2(NO_3)_2]^+$, and (e) $[Am(EtBTP)_3]^{3+}$. Color legend: Am, pink; C, gray; H, white; N, blue; O, red.

dimeric complexes, the average bond distances between the metal center and the O atoms of the nitrate groups are 2.508 and 2.507 Å in the dimeric complexes **1** and **2b**, respectively, and 2.550 and 2.557 Å in the monomeric complexes **2a** and **3**, respectively. The Eu−Eu distances in the dimeric complexes are 4.494 Å in **1** and 4.536 Å in **2b**, i.e., increasing with the size of the alkyl group.

Structures of Molecular Complexes with Eu^{3+} and Am^{3+} Metal Centers and RBTP Ligands. Monomeric molecular complexes with Eu^{3+} and Am^{3+} metal centers and one, two, and three RBTP (R = H, Me, Et) ligands were predicted using DFT based on the information available from spectroscopy experiments. Results for the resulting equilibrium structures of Eu^{3+} and Am^{3+} complexes are shown in Figures 14 and 15, respectively.

Complexes with One RBTP Ligand. The structures of the neutral molecular complexes predicted with DFT included $Am(HBTP)(NO_3)_3$ (**4**), $Eu(HBTP)(NO_3)_3$ (**5**), $Eu(MeBTP)(NO_3)_3$ (**6**), and $Eu(EtBTP)(NO_3)_3$ (**7**). The average Am−N and Am−O bond distances in **4** were predicted to be 2.563 and 2.603 Å. The average Eu−N and Eu−O bond distances are 2.595 and 2.605 Å in **5**, 2.589 and 2.605 Å in **6**, and 2.589 and 2.610 Å in **7**. Unlike in the case of Eu^{3+} complexes constrained in a crystalline environment discussed earlier, the average Eu−N and Eu−O bond distances remain essentially unchanged with the size of the alkyl group.

Complexes with Two RBTP Ligands. The structures of three Am^{3+} complexes and two Eu^{3+} complexes with two RBTP ligands were calculated with DFT, i.e., $[Am(HBTP)_2(NO_3)_2]^+$ (**8**), $[Am(MeBTP)_2(NO_3)_2]^+$ (**9**), $[Am(EtBTP)_2(NO_3)_2]^+$

(10), $[Eu(MeBTP)_2(NO_3)_2]^+$ (11), and $[Eu\text{-}(EtBTP)_2(NO_3)_2]^+$ (12). The average Am—N and Am—O bond distances are predicted to be 2.621 and 2.669 Å in 8, 2.642 and 2.682 Å in 9, and 2.656 and 2.658 Å in 10. In Eu^{3+} complexes, the average Eu—N and Eu—O bond distances are found to be 2.653 and 2.676 Å in 11 and 2.685 and 2.667 Å in 12. Similar to the case of complexes imbedded in a crystal, the average Ln—N bond distances appear to increase with the size of the alkyl groups. It is interesting to note here that when similar Am^{3+} and Eu^{3+} complexes are compared, the Am—N bonds are consistently shorter than the Eu—N bonds in spite of the larger ionic size of Am^{3+} compared to that of Eu^{3+}, whereas the Am—O bonds are marginally larger compared to the Eu—O bonds. This indicates the affinity of these N-donor ligands toward the trivalent actinides over the lanthanides.

Complexes with Three RBTP Ligands. The only structure with three RBTP ligands predicted using DFT was the cationic complex $[Am(EtBTP)_3]^{3+}$ (13). In this complex, the average Am—N bond distance is predicted to be 2.645 Å.

5. CONCLUSIONS

Both ESI-MS and TRLFS studies show consistent results, indicating the formation of higher stoichiometric complexes in the absence of excess nitrate ion, whereas lower stoichiometric complexes are favored in the presence of excess nitrate ion (0.01 M TMAN). The TRLFS study shows different speciation of Eu^{3+} complexes in methanol and acetonitrile media in the presence of 0.01 M TMAN because of stronger nitrate complexation in a poor solvating acetonitrile medium. These combined ESI-MS and TRLFS studies, therefore, gave a clear idea of how the lanthanide complexation of the RBTP ligands changes by changing the R groups and the presence of excess nitrate ion in the medium. From the UV–vis spectrophotometric study, the quantitative idea of the distribution of the different stoichiometric complexes of Ln^{3+} and Am^{3+} with RBTP ligands is obtained in the presence of 0.01 M TMAN by calculating their stability constant values. The tendency to form higher stoichiometric complexes and higher stability constant values for Am^{3+} compared to that of the lanthanides indicates the selectivity of these classes of ligands. The higher affinity of these ligands toward the trivalent actinides over the lanthanides is also reflected in the shorter Am—N bonds compared to the Eu—N bonds from the DFT studies. From the single-crystal XRD study of the Eu^{3+} complexes of the RBTP ligands, dimeric and monomeric complexes were observed with HBTP and EtBTP, respectively, whereas MeBTP forms both monomeric and dimeric complexes. This indicates that a bigger size of the alkyl group favors the formation of a monomeric complex. Higher metal—ligand bond distances with increasing size of the alkyl groups, as observed from single-crystal XRD studies, are supported by the DFT studies. The present work, therefore, provides a clear picture of how the alkyl groups in the RBTP ligands affect their complexation behavior toward An^{3+} and Ln^{3+} in solution and the solid state.

■ ASSOCIATED CONTENT

Ⓢ Supporting Information

X-ray crystallographic data in CIF format, crystal data and structure refinement, atomic coordinates, bond lengths and angles, anisotropic displacement parameters, and hydrogen coordinates and isotropic displacement parameters for 1, 2a, 2b, and 3. This material is available free of charge via the Internet at http://pubs.acs.org.

■ AUTHOR INFORMATION

Corresponding Author

*E-mail: arunasis12@yahoo.co.in.

Notes

The authors declare no competing financial interest.

■ REFERENCES

(1) Choppin, G. R.; Jensen, M. P. Actinides in solution: Complexation and Kinetics. In *The Chemistry of Actinides and Transactinide Elements*, 3rd ed.; Morss, L. R., Edelstein, N. M., Fuger, J., Eds.; Springer: Dordrecht, The Netherlands, 2006; Vol. 4.

(2) Choppin, G. R.; Rizkalla, E. N. Solution Chemistry of Actinides and Lanthanides. In *Handbook on the Physics and Chemistry of Rare Earths*; Gschneidner, K. A., Eyring, L., Eds.; Elsevier: New York, 1994; Vol. 18.

(3) Nash, K. L. *Solv. Extr. Ion Exch.* 1993, 11, 729.

(4) Christiansen, B.; Apostolidis, C.; Carlos, R.; Courson, O.; Glatz, J. P.; Malmbeck, R.; Pagliosa, G.; Romer, K.; Serrano-Purroy, D. *Radiochim. Acta* 2004, 92, 475.

(5) Choppin, G. R. *J. Less Common Met.* 1983, 93, 323.

(6) Madic, C.; Hudson, M. J.; Liljenzin, J. O.; Glatz, J. P.; Nannicini, R.; Facchini, A.; Kolarik, Z. Odoj, R. EUR 19149, European Commission, Luxembourg, 2000.

(7) Kolarik, Z.; Müllich, U.; Gassner, F. *Solv. Extr. Ion Exch.* 1999, 17, 23.

(8) Kolarik, Z.; Müllich, U.; Gassner, F. *Solv. Extr. Ion Exch.* 1999, 17, 1155.

(9) Boucher, C.; Drew, M. G. B.; Giddings, P.; Harwood, L. M.; Hudson, M. J.; Iveson, P. B.; Madic, C. *Inorg. Chem. Commun.* 2002, 5, 596.

(10) Drew, M. G. B.; Guillaneux, D.; Hudson, M. J.; Iveson, P. B.; Russel, M. L.; Madic, C. *Inorg. Chem. Commun.* 2001, 4, 12.

(11) François, N. Ph.D. Thesis, Université Henri Poincaré, Nancy, France, 1999 (CEA-R-5902, 2000).

(12) Smith, R. M.; Martel, A. E. *Critical Stability Constants: Inorganic Ligands*; Plenum Press: New York, 1976; Vol. 4.

(13) Colette, S.; Amekraz, B.; Madic, C.; Berthon, L.; Cote, G.; Moulin, C. *Inorg. Chem.* 2002, 41, 7031.

(14) Colette, S.; Amekraz, B.; Madic, C.; Berthon, L.; Cote, G.; Moulin, C. *Inorg. Chem.* 2004, 43, 6745.

(15) Trumm, S.; Panak, P. J.; Geist, A.; Fanghänel, T. *Eur. J. Inorg. Chem.* 2010, 3022.

(16) Miguirditchian, M.; Guillaneux, D.; Guillaumont, D.; Moisy, P.; Madic, C.; Jensen, M. P.; Nash, K. L. *Inorg. Chem* 2005, 44, 1404.

(17) Denecke, M. A.; Rossberg, A.; Panak, P. J.; Weigl, M.; Schimmelpfennig, B.; Geist, A. *Inorg. Chem.* 2005, 44, 8418.

(18) Denecke, M. A.; Panak, P. J.; Burdet, F.; Weigl, M.; Geist, A.; Klenze, R.; Mazzanti, M.; Gompper, K. *C. R. Chimie* 2007, 10, 872.

(19) Miguirditchian, M.; Guillaneux, D.; François, N.; Airvault, S.; Ducros, S.; Thauvin, D. *Nucl. Sci. Eng.* 2006, 153, 223.

(20) Case, F. H. *J. Heterocycl. Chem.* 1971, 8, 1043.

(21) www.hyperquad.co.uk/HypSpec.htm.

(22) Gans, P.; Sabatini, A.; Vacca, A. *Talanta* 1996, 43, 1739.

(23) Sheldrick, G. M. *Acta Crystallogr., Sect. A* 2008, 64, 112.

(24) Dolomanov, O. V.; Bourhis, L. J.; Gildea, R. J.; Howard, J. A. K.; Puschmann, H. *J. Appl. Crystallogr.* 2009, 42, 339.

(25) Kresse, G.; Furthmüller, J. *Phys. Rev. B* 1996, 54, 11169.

(26) Perdew, P.; Burke, K.; Ernzerhof, M. *Phys. Rev. Lett.* **1996**, *77*, 3865.

(27) Perdew, P.; Wang, J. Y. *Phys. Rev. B* **1992**, *45*, 13244.

(28) Weck, P. F.; Kim, E.; Poineau, F.; Rodriguez, E. E.; Sattelberger, A. P.; Czerwinski, K. R. *Dalton Trans.* **2010**, *39*, 7207.

(29) Blöchl, P. E. *Phys. Rev. B* **1994**, *50*, 17953.

(30) Kresse, G.; Joubert, D. *Phys. Rev. B* **1999**, *59*, 1758.

(31) Davidson, E. R. In *Methods in Computational Molecular Physics*; Diercksen, G. H. F., Wilson, S., Eds.; NATO Advanced Study Institute Series C; Plenum: New York, 1983; Vol. *113*, p 95.

(32) Blöchl, P. E.; Jepsen, O.; Andersen, O. K. *Phys. Rev. B* **1994**, *49*, 16223.

(33) Monkhorst, H. J.; Pack, J. D. *Phys. Rev. B* **1976**, *13*, 5188.

(34) Delley, B. *J. Chem. Phys.* **2000**, *113*, 7756.

(35) Steppert, M.; Walther, C.; Geist, A.; Fanghänel, T. *New J. Chem.* **2009**, *33*, 2437.

(36) Colette, S.; Amekraz, B.; Madic, C.; Berthon, L.; Cote, G.; Moulin, C. *Inorg. Chem.* **2003**, *42*, 2215.

(37) Rawat, N.; Bhattacharyya, A.; Ghosh, S. K.; Gadly, T.; Tomar, B. S. *Radiochim. Acta* **2011**, *99*, 1.

(38) Bruder, V. H.; Haddaoui, J.; Bouhroum, S.; Neu, F. A. *Inorg. Chem.* **2010**, *49*, 1363.

(39) Persson, I. *Pure Appl. Chem.* **1986**, *58* (8), 1153.

(40) Haas, Y.; Stein, G. *J. Phys. Chem.* **1971**, *75* (24), 3668.

(41) Ionova, G.; Rabbe, C.; Guillaumont, R.; Ionov, S.; Madic, C.; Krupa, J.-C.; Guillaneux, D. *New J. Chem.* **2002**, *26*, 234.

(42) Drew, M. G. B.; Guillaneux, D.; Hudson, M. J.; Iveson, P. B.; Madic, C. *Inorg. Chem. Commun.* **2001**, *4*, 462.